Supercontinuum source based on all-silica fibers with optimized spectral power from 1100 up to 2300 nm

J E Saldaña-Díaz[1, 2], S Jarabo[1] and F J Salgado-Remacha[1*]

[1] Universidad de Zaragoza, Departamento de Física Aplicada. Pedro Cerbuna 12, E-50009, Zaragoza, Spain.

[2] Universidad Nacional de Huancavelica, Departamento Académico de Ciencias Básicas, Facultad de Ciencias e Ingeniería, Huancavelica, Perú.

Corresponding author

Francisco Javier Salgado-Remacha. Universidad de Zaragoza, Departamento de Física Aplicada. Pedro Cerbuna 12, E-50009, Zaragoza, Spain; Phone: 34 976 76 10 00; e-mail: fjsalgado@unizar.es

Abstract

The authors present here an attainable fiber supercontinuum source with competitive characteristics in the near infrared range. The proposed system is based on a highly nonlinear silica fiber, with nominal zero-dispersion wavelength at 1550 nm. A mode-locked fiber laser was used as the seed. The pump wavelength was shifted to match the zero-dispersion wavelength of the nonlinear fiber, achieving a better performance of the spectral emission. The supercontinuum emission was characterized between 1100 nm and 2300 nm, showing a flat and wide spectrum with a conversion efficiency over 80%. The set-up consists only in silica fiber and can be considered, therefore, as a cost-effective alternative for supercontinuum generation in the near infrared range, which can be easily implemented in any photonics laboratory, where commercial amplifiers are usual devices.

Keywords: Fibre lasers; Mode-locking; Nonlinear waveguides; Supercontinuum generation.

Highlights

- A supercontinuum source between 1100 and 2300 nm is presented, with optimized flat and wide spectrum.
- The source is based only on silica fibers and commercial devices, resulting in a feasible and easily implemented source.
- The effect of the pump wavelength and the zero-dispersion wavelength is experimentally studied.

1. Introduction

Since its first realization in the early 70s, Supercontinuum (SC) generation continues to be an active topic of research. SC generation requires insertion of optical pulses into a non-linear medium. Different optical sources, such as Er and Er / Yb doped fiber pulsed lasers [1, 2], are used commonly to pump different types of fibers employed as nonlinear media [3-19]. Some applications of SC generation can be found in different fields such as optical coherence tomography, spectral characterization of materials, quantitative analysis of food samples and environment [16-35]. SC with telecommunication devices has received recently considerable boost in attention, as borne out by the references cited. Previously, the authors have developed a new supercontinuum generation source, based on commercial fiber amplifiers [36] and Highly Nonlinear Fibers (HNLF), which gave a spectral width of sufficiently flat profile from 1100 nm up to 2300 nm. This source combines appropriate optical behaviour with cost-effectiveness and feasibility [37]. Nevertheless, there is still room for improvement, particularly in the output spectrum profile.

The spectral width of SC is a key parameter for applying this kind of sources. At the same time, controlling dispersion in the nonlinear medium is somewhat difficult, at present, in the design of SC sources [38]. Although the development of these sources has advanced considerably, there still remains the need to improve their output spectral power and to simplify the dispersion control. Spectral width can be improved in two ways: (i) by raising the pump power of pre-amplification stage or (ii) by shifting the pump wavelength to zero-dispersion wavelength (ZDW) of the HNLF. Since raising the pump power is not always possible, the authors chose suitable pump wavelength for this study.

In their previous work [36], the authors used an L-band Erbium Doped Fiber Amplifier (EDFA) for pre-amplification before the HNLF sample. The resulting spectral power of the SC emission, with the former configuration, showed a spectral hole at 1523 nm. In the present work, we explain and demonstrate how this spectral hole can be overcome by adjusting the pump wavelength making it closer to the spectral hole. Specifically, we have used a C-band EDFA as pre-amplifier before the nonlinear medium, shifting the pumping to the ZDW. This change, in effect, implies that it is a completely new implementation of the source, since it is necessary to calibrate the length of any fiber component that optimizes the output spectrum.

Thus, the present study continues a previous work, but with a new pump configuration for the SC generation source, based on a mode-locking fiber laser used as pumping seed, and HNLF as the dispersive medium. The set-up is based on commercial fiber amplifiers, contributing to attainability and feasibility of the system. The pump wavelength is adjusted to improve the spectral width of the SC generation, using an EDFA in C-band, with 26 dBm of saturation output power. The spectrum of this SC generation source covers from 1100 up to 2330 nm, overcoming an octave-spanning of spectral width. Compared with the previous configuration, the spectral width has been enlarged considerably and, at the same time, a spectral hole appearing in the former output spectrum has been now converted into a ridge. Thus, in this work we show a clear broadening of the SC emission with this kind of devices just by pumping at ZDW of HNLF, based on the same principle that can be found in experimental works reported with photonic crystal fibers (PCF) [38-44], but with a more attainable source. The effect of the pump wavelength and the ZDW has been widely studied in PCF (where the study of the ZDW results much easier) by means of numerical simulations, but this is, up to our knowledge, the first experimental demonstration of the effect in HNLF. This can be considered a significant improvement in the field of SC generation with silica fiber lasers, and eliminates some of the problems present in the former scheme.

2. Experimental set-up

The experimental set-up for the proposed SC generation scheme is shown in Fig. 1. The seed is an all-fiber mode-locked pulsed laser, based on the nonlinear polarization rotation effect. The label EDFA-C20 represents an EDFA operating in the C-band with +20 dBm saturation output power (Highwave, model C20-G20-H-FC/APC-BTO 3.0). The output of the laser is amplified by a second EDFA out of the cavity, acting as pre-amplifier (EDFA-C26), which also operates in the C-band with +26 dBm saturation output power (Manlight, model HWT-EDFA-GM-SC-BO-C26).

The nonlinear medium is a HNLF (Yangtze Optical Fibre and Cable Company Ltd., NL-1550-Zero type). The nominal dispersion parameter D_λ of this fiber at 1550 nm is null, with a dispersion slope lower than 0.025 $ps \cdot nm^{-2} \cdot km^{-1}$ (with $\beta_2 = 2.48 \cdot 10^{-5}$ $ps^2 \cdot km^{-1}$ and $\beta_3 = -2 \cdot 10^{-6}$ $ps^3 \cdot km^{-1}$). The nonlinear coefficient is over 10 $W^{-1} \cdot km^{-1}$ and the Raman gain coefficient is higher than 4.8 W^{-1} km^{-1}. To improve the spectral power of the SC pulses, two fibers were used, one with positive dispersion and the other with negative dispersion; the former is represented by SMF (+) (Corning, model SMF28e) and the latter by SMF (-) (Thorlabs, model DCF38) (see Fig. 1). The optimal fiber lengths for dispersion control were found by maximizing the second harmonic generation, using a BBO crystal, which gives 111 m for the positive dispersion fiber (inside de cavity) and 22 m for the negative dispersion fiber (before the pre-amplification stage). Although these lengths are the same that the ones found in Ref. 37, it was necessary to determine them experimentally again. Moreover, the temporal width of the pulses after the pre-amplifier was measured by means of the interferometric autocorrelation (IAC) method obtaining a value around 0.18 ps, which does not depend on the operation band of the amplifier. Therefore, although the pre-amplifier was changed, it was not necessary to modify these fiber lengths to maximize nonlinear effects. The IAC trace is also shown in Fig. 1. The lateral lobes denote the presence of a substructure in the main pulse, and the flatness of the ground level points to a non-chirped pulse. The peak power reaches around 800 kW (due to the short temporal width of the pulses). Its spectrum is centred at 1561 nm and its frequency of repetition is 1.4 MHz. This frequency depends exclusively on the cavity length, since the laser cavity is based on a passive mode-locking technique.

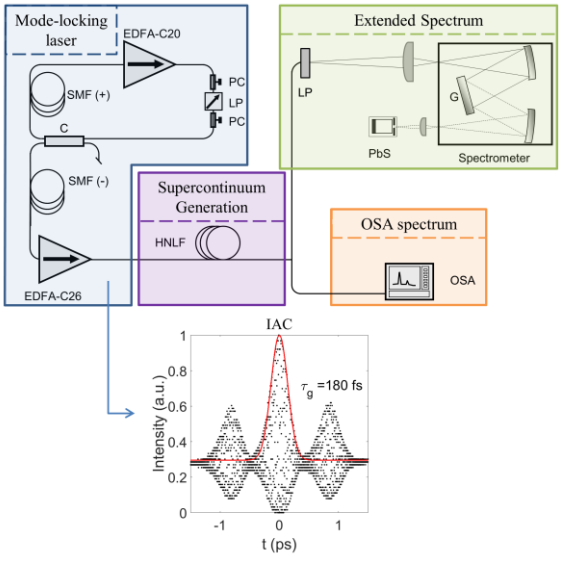

Figure 1. Experimental set-up for supercontinuum generation and measurement. PC: polarization controller; LP: linear polarizer; C: coupler; EDFA-C20/C26: erbium-doped fiber amplifier operating in the C-band (C20: 20 dBm; C26: 26 dBm); SMF (+): single-mode fiber with positive dispersion; SMF (-): single-mode fiber with negative dispersion; HNLF: highly nonlinear silica fiber; OSA: optical spectrum analyser for spectral measurements up to 1700 nm. The spectral measurement range was extended up to 2550 nm by means of a monochromator and a PbS detector; LP: long-pass optical filter; G: diffraction grating. An Interferometric Autocorrelation (IAC) trace of the laser pulse, before the HNLF, is shown, with a temporal Gaussian width of 180 fs.

For spectral measurement, two different arrangements were used. The optical spectrum up to 1700 nm is measured with a spectral resolution of 1 nm by means of an optical spectrum analyser (OSA, Agilent, model 86142B). The spectrum above 1700 nm is obtained with a spectral resolution of 4 nm by using a monochromator (SPEX, model 340E) with a diffraction grating with 300 grooves per millimetre and a Blaze wavelength of 2000 nm (Horiba Scientific) and is detected by means of a PbS photoconductor (spectral sensitivity from 1000 nm up to 2750 nm, Thorlabs, model FDPS3X3). In order to remove the influence of the second diffraction order, a long-pass spectral filter (cut-on wavelength of 1500 nm, Thorlabs, model FEL1500) is placed in front of the photoconductor. A chopper together with a lock-in amplifier allows a synchronous detection. As the spectral efficiency of the diffraction grating depends on the polarization, a linear polarizer is added to the setup. Thus, the optical spectrum is measured for two orthogonal polarizations (vertical and horizontal). Both measurements are corrected using the calibration for each polarization. The final trace is the sum of both measurements and lastly is adjusted in order to match the spectral power obtained with the OSA.

3. Supercontinuum Generation and optimization of the HNLF length

The train of pulses generated by the laser described in the previous section was used as the seed for the generation of SC in the HNLF. To maximize the spectral power of supercontinuum emission, it is necessary to find the optimal length of HNLF. This process is rather laborious, since it involves spectral measurements for both polarizations with different lengths of HNLF. Fig. 2 shows four supercontinuum spectra, pointing out that HNLF of 25 m length gives the maximum spectral width. From this figure it can be seen that we can delimit three clearly different zones: (i) a flat spectral zone from 1134 nm to 1523 nm, (ii) a raised zone between 1523 nm to 1575 nm (which has a higher spectral power) and (iii) a plateau zone from 1575 nm to 2304 nm. The second zone is due to unconverted pump power. As the first and third zones are rather well equalized, it can be assumed that the pump wavelength is close to the ZDW. Unfortunately, the four-wave mixing phase-matching condition cannot be observed due to the silica absorption band around 2300 nm, since the spectrum should extend up to 2680 nm (λ_p = 1560 nm, λ_s = 1100 nm) in order to observe it.

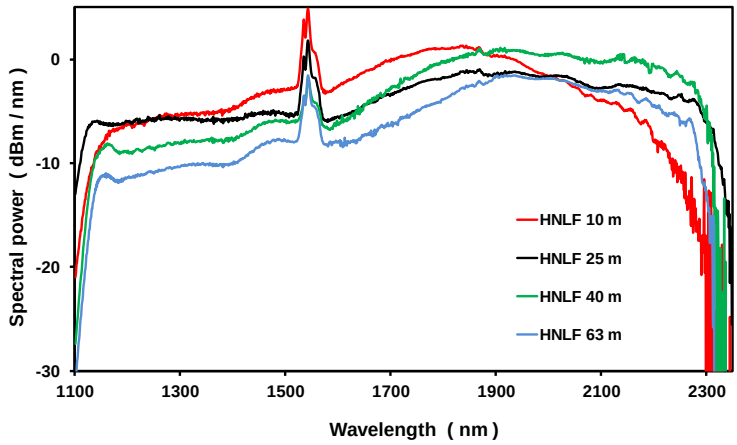

Figure 2. Determination of the optimal HNLF length. The maximum spectral width and maximum total spectral power are found with HNLF of 25 m length. All spectral curves were obtained by employing the highest available pump power.

For a better understanding of the spectral features, Fig. 3 shows the spectral power at four different wavelengths, corresponding to 1101 nm (at the left border of the spectrum), 1200 nm (on the left side of the spectrum), 2190 nm (on the right side) and 2290 nm (at the right border of the spectrum). It can be seen that the optimal length, attending to the maximum power of the whole spectrum, is 25 m. In addition, Fig. 4

shows the maximum and minimum wavelengths for each length of the tested HNLF, taking -11 dBm/nm as the reference power. For the sake of clarity, the inset in Fig 4 shows the curve of spectral width at -11 dBm/nm in greater detail. From this figure, it is obvious that a sample of HNLF of 25 m length produces the widest spectrum, overcoming the octave. Therefore, further discussion on new SC generation scheme would, henceforth, be restricted to this configuration.

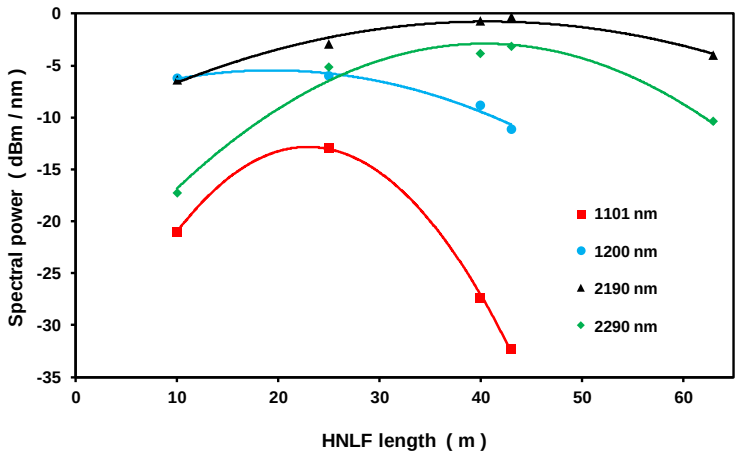

Figure 3. Spectral power at four significant wavelengths (1101 nm, 1200 nm, 2190 nm, and 2290 nm) as a function of HNLF's length. Solid lines are meant for visual aid only. All values were obtained by employing the highest available pump power.

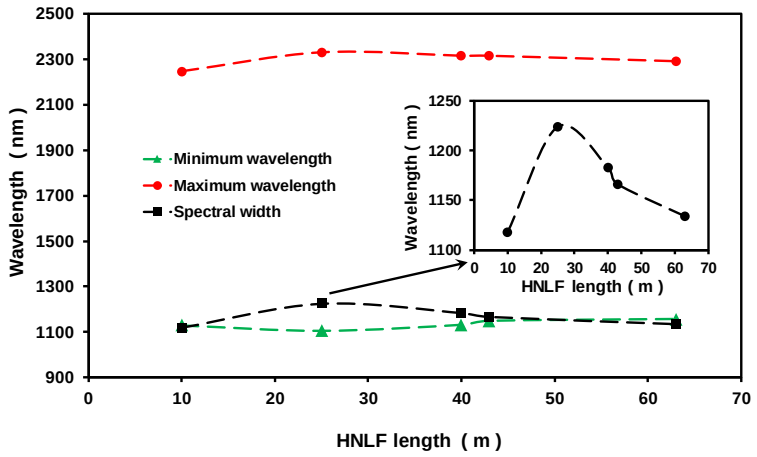

Figure 4. Maximum and minimum wavelengths and spectral width at -11 dBm/nm versus HNLF's length. For clarity, the inset shows the spectral width at -11 dBm/nm as a function of the HNLF length. Dotted curves are meant to be a visual aid only.

The spectral width of supercontinuum (with a HNLF length of 25 m) has its lower limit around 1106 nm, and upper limit at 2330 nm. The spectral power is slightly displaced to the right side of the spectrum (corresponding to longer wavelengths), reaching up to -0.95 dBm with an approximately flat spectrum. Fig. 5 shows the effect of increasing the pump power of the pre-amplifier (EDFA-C26). From this figure, it can be seen that the spectral shape remains the same, regardless of the pump power. The spectral peak surrounding 1550 nm appears even at lower pump powers. It can be concluded, therefore, that this configuration is a

stable source, besides being easy to implement with standard photonics facilities. In fact, by measuring its spectral power during 200 minutes, a stability around ±2% (±0.09 dB) along the whole spectrum in terms of standard deviation has been found. If the measurement time is limited to 15 minutes, its stability improves up to ±1% (±0.04 dB). Therefore, the source is stable enough [45] for a large number of applications, particularly taking into account that OSA measurements are affected on variations around ±0.02dB (during 15 minutes). As an example, the inset in Fig. 5 shows temporal variations of the supercontinuum power at 1300 nm during 200 minutes, showing a standard deviation of ±0.06 dB.

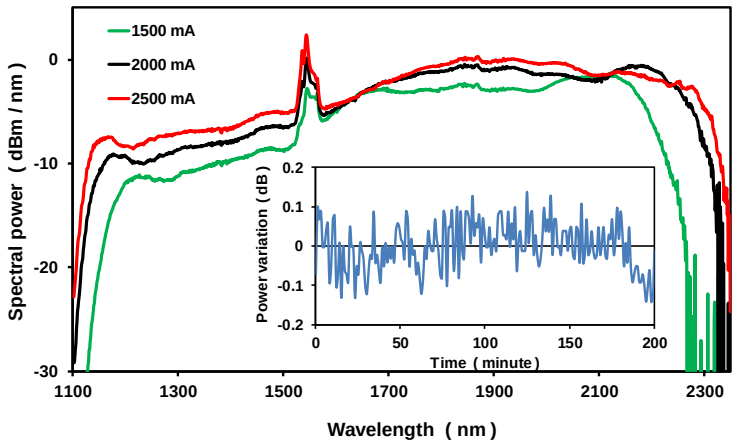

Figure 5. Supercontinuum spectrum generated by 25 m of HNLF pumped with C26 for different pump currents. The inset shows an example of temporal variations of the supercontinuum power at 1300 nm during 200 minutes.

Table 1 collects the spectral widths obtained with the optimal configuration of the system, assuming different minimum powers. From Table 1 can be seen that, taking the spectral width at -6 dBm/nm, it is possible to reach 1170 nm of spectral width (overcoming the octave). Moreover, for -11 dBm / nm (enough for many applications) the spectral width increases up to 1224 nm. This spectral width is really significant, compared with that of other supercontinuum sources as can be seen in the references list. Although wider spectra have been reported, this achievement can be only implemented by using other kind of nonlinear media, reducing therefore the feasibility of the set-up.

Table 1. Spectral widths of the supercontinuum emission generated with 25 meters-long HNLF and spectral widths (in nm) by employing the strongest available pump power.

Minimum power (dBm/nm)	λ_{min} (nm)	λ_{max} (nm)	$\Delta\lambda$ (nm)
-3	1719	2189	470
-6	**1134**	**2304**	**1170**
-11	**1106**	**2330**	**1224**
-13	1101	2336	1235

Finally, it is worthwhile to compare the results obtained from the previous configuration [36] (with a pre-amplifier operating in L-band) with those obtained by using the new solution (by pumping the HNLF with

pulses pre-amplified at C-band). Fig. 6 illustrates the comparison between the spectral powers obtained with both systems. From this figure, it can be seen that pre-amplification at L-band (1600 nm) shows a spectral hole around 1520 nm. This trough in the spectral curve appears even when the pump power is maximum, and it was impossible to eliminate it with the previous configuration. On the contrary, just by shifting the pump wavelength to C-band (1560 nm, closer to the observed spectral hole), the trough could be transformed into a ridge, which is within the spectral region of the pumping source, and therefore can be attached to residual pump power. This effect is due to a better matching between the pump wavelength and the ZDW. In addition, the spectral width is increased, covering from 1106 nm up to 2330 nm over -11 dBm/nm (representing an octave spanning width). At the same time, an increment in the total output power is clear. Moreover, the temporal width of the pulses does not depend on the operation band of the amplifier. Therefore, although the pre-amplifier is changed, it is not necessary to modify the fiber lengths of the pulsed laser. This effect has been widely studied by numerical simulations, and some experimental works [43-44] studied it with PCF (where the ZDW can be easily defined), but this is, up to our knowledge, the first experimental demonstration of the effect based on HNLF.

A comparison between the total spectral power of the C26 pulse and the SC spectrum gives a conversion efficiency around 83% without taking into account the residuary pumping (86% if we take into account the peak at 1545 nm), whereas for the L20 system the efficiency is around 26%. The highest conversion efficiencies has been reported with HNLF in the third window, up to 90% and 80% by Gao et al. [9] and Ouyang et al. [2] respectively. Thus, we reach similar conversion efficiencies. On the other hand, the conversion efficiencies with PCF are below 70% [3, 4, 46], and with other kinds of fibers are below 30% [17, 18, 20].

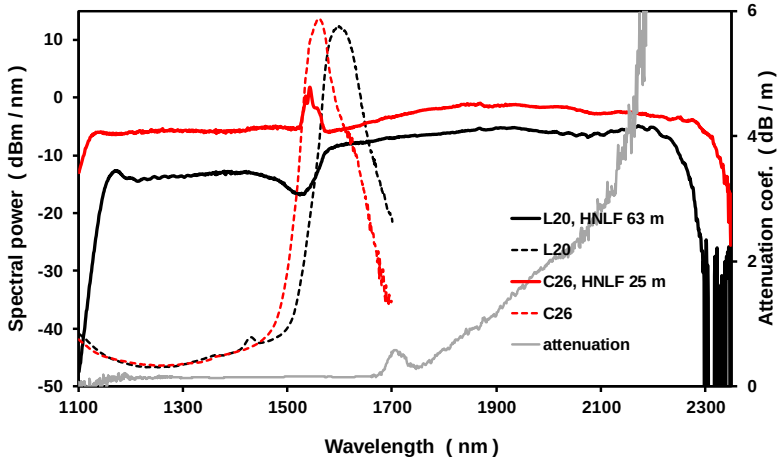

Figure 6. Supercontinuum spectra generated by 25 m (solid red line, EDFA-C26) and 63 m (solid black line, EDFA-L20) of HNLF. Dotted lines show the spectra of the pulsed laser before the HNLF, pre-amplified with C26 (dotted black line) and L20 (dotted grey line); solid grey line: attenuation of the HNLF.

Fig. 6 also shows the attenuation curve for HNLF. As can be seen from this figure, the upper wavelength limit could be reached. Thus, it seems that further significant improvements on the system are hard to implement with silica-based fibers. Note that, therefore, this result cannot be understood as a simple incremental improvement, rather a thorough optimization of the system.

The supercontinuum spectral profiles for both amplifiers (EDFA-L20 and EDFA-C26) were optimized by fitting the HNLF length and the pump power, since the pulsed laser was not modified. However, a great improvement of the supercontinuum profile is found just by amplifying with the EDFA-C26 instead of the

EDFA-L20. Therefore, it is clear that this change is due to the closeness between the pump wavelength and the ZDW of the HNLF. In fact, the nominal ZDW is 1550 nm and the pump wavelength changes from 1600 nm (EDFA-L20) to 1561 nm (EDFA-C26). In order to demonstrate that the improvement shown in this work is due to the control of the dispersion, supercontinuum emission has been also generated by means of a different HNLF (Yangtze Optical Fibre and Cable Company Ltd., NL-1550-Neg type) with negative dispersion parameter D_λ = -5 ps nm^{-1} km^{-1} at 1550 nm. The new profiles are shown in Fig. 7. As the pump wavelengths are out of the ZDW, the supercontinuum is not generated in wavelengths shorter than the pump wavelength and the long wing of the spectrum is narrowed. Finally, a second experiment was carried out by employing again the HNLF-Zero. The pump wavelength can be slightly modified by placing a variable attenuator inside the cavity of the pulsed laser. In Fig. 7 the profile generated with a pump wavelength of 1549 nm is shown and it is clear that this change narrows the supercontinuum profile. Unfortunately, the dispersion of the HNLF changes across the spectrum of the pump pulses (which is very wide) and it is not possible to determine the effective ZDW of the HNLF.

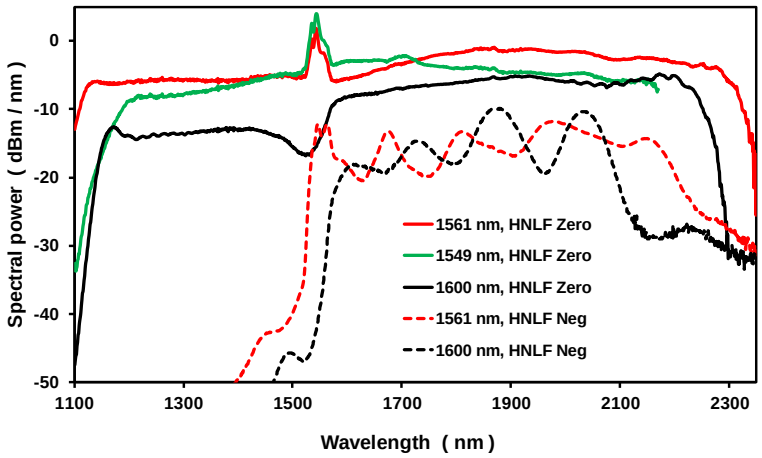

Figure 7. Comparison of different supercontinuum spectra obtained with HNLF-Zero (solid lines) and with HNLF-Neg (dotted lines), pumped at different wavelengths.

Compared with the results obtained by using photonic crystal fibers (PCF) [3-6], highly nonlinear fibers [7-14] or Thulium-based fiber amplifiers [18-20], the development of this new source remains simple and feasible, attaining a competitive spectral width varying between 1100 and 2300 nm. In addition, it develops a considerable amount of power, compared with other supercontinuum sources. Recently, by means of Germanium-doped silica fibers as nonlinear medium, some wider spectra have been reported. These spectra spread from 600 nm to 3200 nm [21, 47] and from 350 nm to 2400 nm [46]. Moreover, its average power is higher, reaching even 80 W [46]. However, their pulses are as long as 1 ns [21, 47] and as 120 ps [46], respectively. Therefore, the spectral peak power of our pulses is around 10 times higher, which can be decisive in some light-matter processes. The flat shape of the spectrum is also noticeable, even compared to commercial devices (see, for example, www.leukos-systems.com or www.nktphotonics.com). The model Fianium Whitelaser (NKT Photonics) has a wider spectrum, from 410 nm to 2400 nm, and its spectral average power is around 10 times higher that our SC spectrum. However, the temporal width of its pulses is around 1 ps and the output power is not coupled in an optical fiber, with a 2.5 mm spot diameter, which diminishes strongly the output optical intensity. The average power of the model Samba (Leukos Systems) with fiber output (instead of collimator output) is similar to the one of our device, but its pulses last 1 ns. Further enlargement of this spectral curve would be possible only with the use of other nonlinear materials:

ZBLAN fibers [15-17] or Germanium-doped fibers [21, 46-47], but this reduces the feasibility of attaining the source.

4. Conclusions

A new alternative is presented for supercontinuum generation in highly nonlinear silica fibers, pumped by Er-doped-fiber mode-locked lasers. The pump wavelength has been shifted closer to the ZDW of the nonlinear medium. Compared with a former configuration, the one proposed here eliminates the presence of a spectral hole in the output spectrum, besides enlarging considerably the spectral width. The following are the main advantages of the proposed system: feasibility for practical use, attainability and cost-effectiveness (advantageous in volume production and cost control), good stability for the output power, and broad spectrum with competitive flatness. We also present the supercontinuum spectra obtained with different pump wavelengths and for different ZDW, demonstrating the importance of choosing the right pump wavelength, depending on the nonlinear medium.

The supercontinuum spectrum was characterized by means of an OSA and a monochromator, combined with a PbS detector. The resulting spectral curve shows a flat profile between 1100 nm and 2300 nm over -11 dBm/nm with a conversion efficiency above 80%. Compared with more complex solutions (based, for example, on photonic crystal fibers or Thulium-based fiber amplifiers), the proposed set-up is simple and feasible with a very competitive performance. Therefore, it can be easily implemented using commercial erbium-doped amplifiers. Any attempt to markedly improve this set-up would be fraught with complications, because of the spectral attenuation of HNLF. Thus, for a wider enlargement, a different medium like ZBLAN fibers or Germanium-doped fibers would be required, resulting in a not easily attainable source. The solution presented in this work points out the importance of properly shifting the pump to the nominal ZDW of the nonlinear medium and it can be very helpful for the research of supercontinuum sources in the near-infrared region. Although numerical simulations of this effect have been widely reported and there are a few experimental works [43-44] that demonstrate it by sweeping the pump wavelength in PCF with ZDW around 1550 nm, this one is, up to our knowledge, the first experimental demonstration pumping a HNLF in 1550 nm of the upgrade of the SC spectrum by means of matching the pump wavelength and the ZDW of the HNLF.

Acknowledgements

This work was supported by the Ministerio de Economía y Competitividad (Programa Estatal de Fomento de la Investigación Científica y Técnica de Excelencia, project FIS2013-44174-P) and by the Diputación General de Aragón.

J E Saldaña-Díaz acknowledges the financial support of Universidad de Zaragoza and Banco Santander (Doctoral Fellowship UZ-SANTANDER).

References

[1] R. R. Alfano, The Supercontinuum Laser Source: Fundamentals with Updated References, New York NY, ed Springer, 2006, pp. 33-90.

[2] D. Q. Ouyang, G. Y. Guo, S. C. Ruan, P. G. Yan, H. F. Wei and J. Luo, “Optimized flat supercontinuum generation in high nonlinear fibers pumped by a nanosecond Er/Yb Co-doped fiber amplifier,” Laser Phys., 24 (2014) 045104.

[3] A. Jin, H. Zhou, X. Zhou, J. Hou, Z. Jiang, "High-Power Ultraflat Near-Infrared Supercontinuum Generation Pumped by a Continuous Amplified Spontaneous Emission Source," IEEE Photon. J., 7 (2015) 1600409.

[4] S. Gao, Y. Wang, R. Sun, H. Li, C. Tian, D. Jin and P. Wang, "Ultraviolet-enhanced supercontinuum generation in uniform photonic crystal fiber pumped by a giant-chirped fiber laser," Opt. Express, 22 (2014) 24697-24705.

[5] M. Klimczak, B. Siwicki, P. Skibinski, D. Pysz, R. Stepien, A. Heidt, C. Radzewick and R. Buczynski, "Coherent supercontinuum generation up to 2.3 μm in all-solid soft-glass photonic crystal fibers with flat all-normal dispersion," Opt. Express, 22 (2014) 18824-8832.

[6] A. Labruyère, A. Tonello, V. Couderc, G. Huss and P. Leproux, "Compact supercontinuum sources and their biomedical applications," Opt. Fiber Technol., 18 (2012) 375-378.

[7] S. S. Lin, S. K. Hwang and J. M. Liu, "Supercontinuum generation in highly nonlinear fibers using amplified noise-like optical pulses," Opt. Express, 22 (2014) 4152-4160.

[8] S. Rui, H. Jing, W. Ze-Feng, X. Rui and L. Qi-Sheng, "Effect of initial chirp on near-infrared supercontinuum generation by a nanosecond pulse in a nonlinear fiber amplifier," Chin. Phys. B, 22 (2013) 084206.

[9] W. Gao, M. Liao, X. Yan, T. Suzuki and Y. Ohishi, "All-fiber quasi-continuous wave supercontinuum generation in single-mode high-nonlinear fiber pumped by submicrosecond pulse with low peak power," Appl. Opt., 51 (2012) 2346-2350.

[10] N. Nishizawa, "Generation and application of high-quality supercontinuum sources," Opt. Fiber Technol., 18 (2012) 394-402.

[11] V. A. Kamynin, A. S. Kurkov and V. M. Mashinsky, "Supercontinuum generation up to 2.7 μm in the germanate-glass-core and silica-glass-cladding fiber," Laser Phys. Lett., 9 (2012) 219-222.

[12] J. Swiderski and M. Maciejewska, "Watt-level, all-fiber supercontinuum source based on telecom-grade fiber components," Appl. Phys. B, 109 (2012) 177-181.

[13] C. Xia, M. Kumar, M. Y. Cheng, O. P. Kulkarni, M. N. Islam, A. Galvanauskas, F. L. Terry, M. J. Freeman, D. A. Nolan and W. A. Wood, "Supercontinuum Generation in Silica Fibers by Amplified Nanosecond Laser Diode Pulses," IEEE J. Sel. Top. Quantum Electron., 13 (2007) 789-797.

[14] J. W. Nicholson, A. D. Yablon, P. S. Westbrook, K. S. Feder and M. F. Yan, "High power, single mode, all-fiber source of femtosecond pulses at 1550 nm and its use in supercontinuum generation," Opt. Express, 12 (2004) 3025-3034.

[15] A. M. Heidt, J. H. V. Price, C. Baskiotis, J. S. Feehan, Z. Li, S. U. Alam and D. J. Richardson, "Mid-infrared ZBLAN fiber supercontinuum source using picosecond diode-pumping at 2 μm," Opt. Express, 21 (2013) 24281-24287.

[16] S. Dupont, C Petersen, J. Thogersen, C. Agger, O. Bang and S. R. Keiding, "IR microscopy utilizing intense supercontinuum light source," Opt. Express, 20 (2012) 4887-4892.

[17] M. Kumar, M. N. Islam, F. L. Terry, M. J. Freeman, A. Chan, M. Neelakandan and T. Manzur, "Stand-off detection of solid targets with diffuse reflection spectroscopy using a high-power mid-infrared supercontinuum source," App. Opt., 51 (2012) 2794-2807.

[18] V. Dvoyrin and I. T. Sorokina, "6.8 W all-fiber supercontinuum source at 1.9–2.5 μm," Laser Phys. Lett., 11 (2014) 085108.

[19] V. V. Alexander, Z. Shi, M. N. Islam, K. Ke, M. J. Freeman, A. Ifarraguerri, J. Meola, A. Absi, J. Leonard, J. Zadnik, A. S. Szalkowski and G. J. Boer, "Power scalable >25 W supercontinuum laser from 2 to 2.5 μm with near-diffraction-limited beam and low output variability," Opt. Lett., 38 (2013) 2292-2294,.

[20] G. Xue, B. Zhang, W. Yan, K. Yin and J. Hou, "Stable high-spectral-flatness mid-infrared supercontinuum generation in Tm-doped fiber amplifier," Opt. Fiber Technol., 24 (2015) 1-4.

[21] L. Yang, B. Zhang, K. Yin, J. Yao, G. Liu and J. Hou, "0.6-3.2 μm supercontinuum generation in a step-index germania-core fiber using a 4.4 kW peak-power pump laser," Opt. Express, 24 (2016) 12600-12606.

[22] L. Shi, L. A. Sordillo, A. Rodríguez-Contreras and R. Alfano, "Transmission in near-infrared optical windows for deep brain imaging," J. Biophotonics, 9 (2016) 38-43.

[23] C. S. Cheung, J. M. O. Daniel, M. Tokurakawa, W. A. Clarkson and H. Liang, "High resolution Fourier domain optical coherence tomography in the 2 μm wavelength range using a broadband supercontinuum source," Opt. Express, 23 (2015) 1992-2001.

[24] T. Gottschall, T. Meyer, M. Baumgartl, C. Jáuregui, M. Schmitt, J. Popp, J. Limpert and A. Tunnermann, "Fiber-based light sources for biomedical applications of coherent anti-Stokes Raman scattering microscopy," Laser Photonics Rev., 9 (2015) 435-451.

[25] M. Yamanaka, H. Kawagoe and N. Nishizawa, "High-speed ultrahigh-resolution spectral domain optical coherence tomography using high-power supercontinuum at 0.8 μm wavelength," Appl. Phys. Express, 9 (2015) 022701.

[26] H. Pires, M. Baudisch, D. Sánchez, M. Hemmer and J. Biegert, "Ultrashort pulse generation in the mid-IR," Prog. Quant. Electron., 43 (2015) 1-30.

[27] L. A. Sordillo, L. Lindwasser, Y. Budansky, P. Leproux and R. Alfano, "Near-infrared supercontinuum laser beam source in the second and third near-infrared optical windows used to image more deeply through thick tissue as compared with images from a lamp source," J. Biomed. Opt., 20 (2015) 030501.

[28] A. N. Tsypkin, S. E. Putilin, A. V. Okishev and S. A. Kozlov, "Ultrafast information transfer through optical fiber by means of quasidiscrete spectral supercontinuums," Opt. Eng., 54 (2015) 056111,.

[29] T. Werblinski, F. Mittmann, M. Altenhoff, T. Seeger, L. Zigan and S. Will, "Temperature and water mole fraction measurements by time-domain-based supercontinuum absorption spectroscopy in a flame," Appl. Phys. B, 118 (2015) 153-158.

[30] H. Kawagoe, S. Ishida, M. Aramaki, Y. Sakakibara, E. Omoda, H. Kataura and N. Nishizawa, "Development of a high power supercontinuum source in the 1.7 μm wavelength region for highly penetrative ultrahigh-resolution optical coherence tomography," Biomed. Opt. Express, 5 (2014) 932-943.

[31] I. Korel, B. N. Nyushkov, V. I. Denisov, V. S. Pivtsov, N. Koliada, A. A. Sysoliatin, S. M. Ignatovich, N. L. Kvashnin, M. N. Skvortsov and S. N. Bagayev, "Hybrid highly nonlinear fiber for spectral supercontinuum generation in mobile femtosecond clockwork," Laser Phys., 24 (2014) 074012.

[32] N. Nishizawa, "Ultrashort pulse fiber lasers and their applications," Jpn. J. Appl. Phys., 53 (2014) 090101.

[33] J. Swiderski, "High-power mid-infrared supercontinuum sources: Current status and future perspectives," Prog. Quant. Electron., 38 (2014) 189-235.

[34] L. J. Medhurst, "FTIR determination of pollutants in automobile exhaust: An environmental chemistry experiment comparing cold-start and warm-engine conditions," J. Chem. Educ., 82 (2005) 278-281.

[35] J. Chalmers and P. Griffiths, Handbook of Vibrational Spectroscopy: Theory and Instrumentation, Vol 1, Chichester UK, ed John Wiley & Sons Ltd, 2002, pp. 256-272

[36] J. E. Saldaña-Díaz, S. Jarabo and F. J. Salgado-Remacha, “Octave-spanning supercontinuum generation in highly nonlinear silica fibres based on cost-effective fibre amplifiers,” Laser Phys. Lett., 13 (2016) 095102.

[37] J. E. Saldaña-Díaz, S. Jarabo, F. J. Salgado-Remacha, L. Perdices, I. Pinilla, and A. Sánchez-Cano, “Spectral attenuation of brain and retina tissues in the near-infrared range measured using a fiber-based supercontinuum device,” J. Biophotonics 10 (2017) 1105-1109.

[38] J. M. Dudley, G. Genty, and S. Coen, “Supercontinuum generation in photonic crystal fiber,” Rev. Mod. Phys. 78 (2006) 1135-1184.

[39] G. Genty, M. Lehtonen, and H. Ludvigsen, "Enhanced bandwidth of supercontinuum generated in microstructured fibers," Opt. Express 12 (2004) 3471-3480.

[40] L. Tartara, I. Cristiani, and V. Degiorgio, "Blue light and infrared continuum generation by soliton fission in a microstructured fiber," Appl. Phys. B 77 (2003) 307-311.

[41] A. Ortigosa-Blanch, J. C. Knight, and P. St. J. Russell, "Pulse breaking and supercontinuum generation with 200-fs pump pulses in photonic crystal fibers," J. Opt. Soc. Am. B 19 (2002) 2567-2572.

[42] B. R. Washburn, S. E. Ralph, and R. S. Windeler, "Ultrashort pulse propagation in air-silica microstructure fiber," Opt. Express 10 (2002) 575-580.

[43] W. H. Reeves, D. V. Skryabin, F. Biancalana, J. C. Knight, P. St. J. Russell, F. G. Omenetto, A. Efimov, and A. J. Taylor, "Transformation and control of ultrashort pulses in dispersion-engineered photonic crystal fibres," Nature 424 (2003) 511-515.

[44] A. B. Fedotov, A. N. Naumov, A. M. Zheltikov, I. Bugar, D. Chorvat Jr., D. Chorvat, A. P. Tarasevitch, and D. von der Linde, "Frequency-tunable supercontinuum generation in photonic-crystal fibers by femtosecond pulses of an optical parametric amplifier," J. Opt. Soc. Am. B 19 (2002) 2156-2164.

[45] A. Kudlinski, B. Barviau, A. Leray, C. Spriet, L. Héliot, and A. Mussot, "Control of pulse-to-pulse fluctuations in visible supercontinuum," Opt. Express 18 (2010) 27445-27454.

[46] X. Qi, S. Chen,Z. Li, T. Liu, Y. Ou, N. Wang, and J. Hou, "High-power visible-enhanced all-fiber supercontinuum generation in a seven-core photonic crystal fiber pumped at 1016 nm, " Opt. Lett. 43 (2018) 1019-1022.

[47] D. Jain, R. Sidharthan, P. M. Moselund, S. Yoo, D. Ho, and O. Bang, "Record power, ultra-broadband supercontinuum source based on highly GeO2 doped silica fiber," Opt. Express 24 (2016) 26667.